`

Advanced Real-time Simulation of Single-Phase Flow in Heated Pipes: A Novel Mathematical Method for Dynamic Heat Transfer Modeling

Baoxiang Zhang [a], Haifeng Xu [b], Hongying Li [a], Shuangli Yao [a], and Xiaohu Xu [c]*

(https://orcid.org/0000-0002-8843-0173)

[a] *Tangshan Sanyou Chemical Industries Co. Ltd. Thermal Power Branch, Hebei 063020, China*

[b] *Nanjing Pankong Energy technology Co. Ltd., Nanjing 211135, China*

[c] *National Engineering Research Center of Power Generation Control and Safety, School of Energy and Environment, Southeast University, Nanjing 210096, China*

**e-mail: 101010376@seu.edu.cn*

Abstract— In this study, we proposed a dynamic heat transfer model for the thermal simulation of single-phase flow in heated pipes, which are widely used in industrial applications such as power plants, renewable energy systems, and other forced convection systems. At present, the proposed model achieves real-time calculations relied on lumped parameter models (LPM). While distributed parameter models (DPM) offered a better computational accuracy. Unlike traditional LPMs, which often oversimplify transient dynamics, our model incorporates a dynamic heat transfer equation with explicit variable representation, allowing for explicit time-marching calculations. Comparative analyses with DPMs and LPMs demonstrate that our model achieves higher accuracy than LPMs while maintaining computational efficiency suitable for real-time applications. This advancement addresses the limitations of existing methods, providing a cost-effective and precise solution for simulating heated pipe dynamics under transient conditions. Engineering applications could benefit from this study by incorporating the model as part of simulators for real-time optimization of thermal systems, such as single-phase heat transfer sections in power plant boilers and industrial systems. Future prospects include extending the model to water and superheated steam segments in two-phase flow, further improving its computational efficiency and applicability in complex industrial scenarios through moving boundary modeling.

Keywords: single-phase flow heated pipes, mathematical model, lumped parameters, distributed parameters, simulator

1. INTRODUCTION

Heated pipes, externally warmed or cooled by outside sources and not generating heat itself, are employed in industrial settings to raise or decrease the temperature of working fluid for further processing. Their applications range from enhancing energy efficiency through improved waste heat recovery [1-3] to maintaining essential temperatures in coal-fired power plant equipment [4-6]. Additionally, heated pipes play a crucial role in renewable energy sectors, particularly in solar plant systems [7-9]. In electric vehicles, they improve performance and extend battery life by effectively

`

managing heat dissipation [10-13]. In electronics, heated pipes are vital for maintaining optimal component temperature, crucial for system performance and longevity [14-17]. The effectiveness of heated pipes hinges on the heat transfer between the tube wall and the working fluid, a critical aspect regardless of the heated pipes' design or the phase of the working fluid. Recent studies have demonstrated that nanofluids, as a passive heat transfer enhancement method, significantly improve thermal conductivity, heat transfer rates, and energy efficiency in heat exchangers, with their performance influenced by factors such as nanoparticle concentration, Reynolds number, and particle size, while geometric optimizations like rib turbulators and finned tubes further amplify heat transfer efficiency, making them highly effective for industrial applications [18-28].

The simulation of heat dissipation in heated pipes predominantly adopts the distributed parameter model (DPM) approach, using computational fluid dynamics (CFD) for in-depth analysis [4, 15]. In contrast, simulator of heated pipes often relies on a lumped parameter model (LPM) simplified for fast real-time computation [29]. CFD is essential for simulating heat dissipation and fluid dynamics in heated pipes, enabling precise predictions of spatial temperature distribution and heat transfer, which inform design optimizations and enhance performance and energy efficiency. While CFD is adept at simulating the complex behaviors of fluid flow within heated pipes, it is not always the most efficient for real-time simulation system. Here, simplified LPMs offer a more computationally efficient alternative. LPMs reduce the complexity of heated pipes systems to manageable levels by conceptualizing them as assemblies of interconnected nodes with averaged behaviors. This simplification aids in developing simulation strategies that enable real-time optimization.

Currently, real-time simulation systems are primarily used to simulate production processes (both normal and fault conditions), requiring the simulator to replicate actual dynamic processes at a 1:1 scale or even faster. This means that the dynamic mathematical models developed for simulators must appropriately simplify internal flow process details. For single-phase heated pipes (SFHPs), these simplifications include: (1) assuming that the dynamic characteristics of parallel heated pipes are identical, so the modeling only requires developing a dynamic mathematical model for a single heated pipe; (2) considering that the fluid properties within the pipe vary only along the axial (length) direction, while ignoring radial non-uniformity, thereby simplifying the three-dimensional flow of the fluid to one-dimensional flow; and (3) dividing the pipe into several control volumes of equal length along the axial direction and treating the outlet parameters of each control volume as lumped parameters. Due to real-time constraints, the number of control volumes is limited, making it highly meaningful to improve the accuracy of the model for each control volume. In this study, we introduced a hybrid model integrating analytical and numerical solutions (HM-AN) to simulate the dynamic heat transfer process of SFHPs. This study is significant as it bridges the gap between computational efficiency and simulation accuracy, providing a practical solution for real-time thermal modeling of single-phase flow heated pipes, which are critical components in industrial systems such as power plants, renewable energy systems, and advanced heat exchangers.

The core innovation and algorithmic novelty of this model include, firstly, the implementation of an explicit convergence solution that quickly accounts for the heat reservoir of the tube wall from the outside and the thermal release to the inside working fluid. This dynamic approach marks a departure from previous LPM, which relied on steady-state formulas to address the heat transfer from the tube

`

wall to the internal fluid [30]. Secondly, we derived Laplace transfer functions for the three models (LPM, DPM, and HM-AN) and conducted a theoretical comparison of the calculation errors among them. Lastly, we performed simulations of dynamic disturbances across all three models to assess their adaptability to varying conditions of thermal supply and demand. Operational simulations under specific scenarios were executed, considering disturbance input parameters such as inlet temperature, velocity of flow, and external heat duty, to evaluate the models' performance under these varying conditions.

2. MATHEMATICAL MODEL

2.1 A NEW DYNAMIC ANALYSIS OF HEAT RESORSE

In Fig. 1, water/steam is depicted as a single-phase substance flowing through a single-phase SFHP unit. As it traverses the unit, it absorbs heat from the metal wall. Given the constrained length of the unit, physical parameters within it may be considered either constant or linear. Despite potential inhomogeneities in the physical properties of the fluid along the tube wall, it's possible to individually define the physical parameters for the fluid within each discretized unit. The mass and energy balance equations for the system are presented as follows:

$$\frac{\partial D}{\partial z} + F\frac{\partial \rho}{\partial \tau} = 0 \quad (1)$$

$$q_2 = D\frac{\partial h}{\partial z} + F\rho\frac{\partial h}{\partial \tau} - F\frac{\partial p}{\partial \tau} \quad (2)$$

Drawing upon principles from fluid mechanics, the heat transfer from the tube wall to the fluid across the entire unit is computed as follows:

$$q_2 = \alpha_2 \pi d_2 (T_j - T) = \alpha_2 U_2 (T_j - T) \quad (3)$$

The momentum balance is expressed as:

$$\frac{\partial p}{\partial z} + p_d = 0 \quad (4)$$

The equation for the state of the fluid is presented as:

$$\rho = \rho(p, T) \quad (5)$$

$$h = h(p, T) \quad (6)$$

Lastly, the heat balance equation for the tube unit is articulated as:

$$q_1 - q_2 = m_j c_j \frac{dT_j}{d\tau} \quad (7)$$

In Eq. (7), for a given unit along the *z*-direction, the temperature of the tube wall is assumed to be constant. $\partial T_j / \partial z = 0$ .The heat transfer initiates from the external heat source to the metal tube wall. In this context, q_1 is considered a convenient boundary condition that encapsulates heat transfer components as described in the outer equations [19].

From Eq. (6), we derive the following expressions:

$$\frac{\partial h}{\partial z} = \left(\frac{\partial h}{\partial T}\right)_p \frac{\partial T}{\partial z} + \left(\frac{\partial h}{\partial p}\right)_T \frac{\partial p}{\partial z} = c_p \frac{\partial T}{\partial z} - \left(\frac{\partial h}{\partial p}\right)_T p_d \quad (8)$$

`

$$\frac{\partial h}{\partial \tau} = c_p \frac{\partial T}{\partial \tau} + \left(\frac{\partial h}{\partial p}\right)_T \frac{\partial p}{\partial \tau} \quad (9)$$

Upon substituting Eq. (8) and (9) into Eq. (2), we arrive at:

$$\alpha_2 U_2 (T_j - T) = Dc_p \frac{\partial T}{\partial z} - Dp_d \left(\frac{\partial h}{\partial p}\right)_T + F\rho c_p \frac{\partial T}{\partial \tau} + F\left(\rho\left(\frac{\partial h}{\partial p}\right)_T - 1\right)\frac{\partial p}{\partial \tau} \quad (10a)$$

With the given conditions for $\partial T_j / \partial z = 0$ and the flow formula $D = F\rho\omega$, we obtain:

$$\frac{\partial (T_j - T)}{\partial z} + \frac{\alpha_2 U_2}{Dc_p}(T_j - T) = \frac{1}{\omega}\frac{\partial T}{\partial \tau} - \frac{p_d}{c_p}\left(\frac{\partial h}{\partial p}\right)_T + \frac{F}{Dc_p}\left(\rho\left(\frac{\partial h}{\partial p}\right)_T - 1\right)\frac{\partial p}{\partial \tau} \quad (10b)$$

Given the observation that the dynamic process of flow responding to changes in pressure occurs at a significantly faster rate compared to the process of enthalpy responding to temperature changes, it is commonly assumed that the flow-pressure dynamic has stabilized by the time enthalpy-temperature calculations are performed, leading to the conclusion that $\partial p / \partial \tau = 0$. Furthermore, it is assumed that pressure within a unit is uniformly distributed along its length, p_d=0. Consequently, we obtain:

$$\frac{\partial (T_j - T)}{\partial z} + \frac{\alpha_2 U_2}{Dc_p}(T_j - T) = \frac{1}{\omega}\frac{\partial T}{\partial \tau} \quad (11)$$

At time τ, the spatial integration along the pipe length L is performed, and the outlet temperature, T_{out}, is used as a lumped parameter to represent the rate of temperature change. According to the boundary condition $(T_j - T)_{z=0} = T_j - T_{in}$, we obtain:

$$T_{out} = T_j - \frac{L}{\omega}\frac{Dc_p}{\alpha_2 A_2}\frac{dT_{out}}{d\tau} - \left(T_j - T_{in} - \frac{L}{\omega}\frac{Dc_p}{\alpha_2 A_2}\frac{dT_{out}}{d\tau}\right)e^{-\frac{\alpha_2 A_2}{Dc_p}} \quad (12)$$

Where A_2 represents the inner surface area of the entire tube unit, which, when integrated along the z-direction, equates to $U_2 L$.

By integrating Eq. (3) and (11), we further derive the following result:

$$Q_2 = Dc_p \frac{L}{\omega}\frac{dT_{out}}{d\tau} + Dc_p\left(T_j - T_{in} - \frac{L}{\omega}\frac{Dc_p}{\alpha_2 A_2}\frac{dT_{out}}{d\tau}\right)\left(1 - e^{-\frac{\alpha_2 A_2}{Dc_p}}\right) \quad (13)$$

Similarly, by integrating Equation (7) along the pipe length L, the dynamic equation for the heated pipe wall temperature is obtained.

$$Q_1 - Q_2 = m_j c_j L \frac{dT_j}{d\tau} \quad (14)$$

Here, Q_1 represents the heat released by the external heating fluid to the heated pipe, where $Q_1 = q_1 L$.

Eq. (12), (13), and (14) form a new dynamic mathematical model for the SFHP, where Q_2 represents the time-dependent heat release affecting the temperature change of the fluid inside. This model aligns with the steady-state results obtained from both the LPM and DPM, yet it introduces a dynamic calculation formula not previously deduced as the derivative of T_j with respect to time. In engineering contexts, Delay Partial Differential Equations (DPDEs) are employed within simulation and networked systems, where delays can lead to instability or impact system performance [31-33].

`

This suggests that by identifying the key variables influencing system delays through mathematical modeling, we can design simulating strategies to enhance system efficiency.

When the fluid temperature within the model reaches a steady state, $dT_{out}/d\tau = 0$. By integrating Eq. (12) and (13), we can derive the following result:

$$T_{out0} = T_{j0} - (T_{j0} - T_{in0})e^{-\frac{\alpha_{20}A_2}{D_0 c_{p0}}} \quad (15)$$

$$Q_{20} = D_0 c_{p0}(T_{j0} - T_{in0})(1 - e^{-\frac{\alpha_{20}A_2}{D_0 c_{p0}}}) \quad (16)$$

The subscript 0 denotes the steady-state parameter. In order to distinguish the coefficients and variables which to be solved as $dT_{out}/d\tau$, $dT_j/d\tau$ and Q_2, we defined $\mathbf{A}\,y = S$ in the form of matrix as the following:

$$\mathbf{A} = \begin{bmatrix} \frac{L}{\omega}\frac{Dc_p}{\alpha_2 A_2}(1 - e^{-\frac{\alpha_2 A_2}{Dc_p}}) & 0 & 0 \\ Dc_p \frac{L}{\omega}\left(1 - \frac{Dc_p}{\alpha_2 A_2}(1 - e^{-\frac{\alpha_2 A_2}{Dc_p}})\right) & 0 & -1 \\ 0 & M_j c_j & 1 \end{bmatrix}$$

$$y = \begin{bmatrix} \frac{\partial T_{out}}{\partial \tau} \\ \frac{\partial T_j}{\partial \tau} \\ Q_2 \end{bmatrix}, \quad S = \begin{bmatrix} (1 - e^{-\frac{\alpha_2 A_2}{Dc_p}})T_j + e^{-\frac{\alpha_2 A_2}{Dc_p}} T_{in} - T_{out} \\ -Dc_p(1 - e^{-\frac{\alpha_2 A_2}{Dc_p}})(T_j - T_{in}) \\ Q_1 \end{bmatrix}$$

Where $M_j = m_j L$.

To address the effects of fluid specific heat and the absorbed heat of the tube wall, it is essential to incorporate the physical property continuity equations into the models. Drawing on the concept of traditional multi-stage lumped parameter modeling, the heated tube is segmented along its length, with the physical model of one segment depicted in Fig. 2.

The rate of change of density with respect to time is represented as follows:

$$\frac{\partial \rho}{\partial \tau} = \left(\frac{\partial \rho}{\partial p}\right)_T \frac{\partial p}{\partial \tau} + \left(\frac{\partial \rho}{\partial T}\right)_p \frac{\partial T}{\partial \tau} \quad (17)$$

Substituting Eq. (17) into Eq. (1) leads to the derivation of the fluid continuity equation as follows:

$$\left.\begin{aligned} \frac{FL}{N}\left(\frac{\partial \rho_{i+1}}{\partial T_{i+1}}\right)_P \frac{dT_{i+1}}{d\tau} + D_{i+1} &= D_{in} - \frac{FL}{N}\left(\frac{\partial \rho_{i+1}}{\partial p}\right)_{T_{i+1}} \frac{dp}{d\tau}, & i = 0 \\ \frac{FL}{N}\left(\frac{\partial \rho_{i+1}}{\partial T_{i+1}}\right)_P \frac{dT_{i+1}}{d\tau} - D_i + D_{i+1} &= -\frac{FL}{N}\left(\frac{\partial \rho_{i+1}}{\partial p}\right)_{T_{i+1}} \frac{dp}{d\tau}, & i > 0 \end{aligned}\right\} \quad (18)$$

`

Eq. (18), (12), (13), and (14) collectively form a hybrid model that accounts for changes in physical properties. The parameters to be determined for each segment of the model include the output fluid temperature, the metal wall temperature, the mass flow, and the heat transfer from the tube wall to the fluid, all expressed in explicit forms. When the heated tube is divided into continuous segments, the parameter vector y to be solved comprises a total of 4*N* elements, where *N* is the number of segments.

$$y=\left\{\frac{\partial T_1}{\partial \tau},\frac{\partial T_2}{\partial \tau},...\frac{\partial T_n}{\partial \tau},\frac{\partial T_{j,0}}{\partial \tau},\frac{\partial T_{j,1}}{\partial \tau},...,\frac{\partial T_{j,n-1}}{\partial \tau},D_1,D_2,...,D_n,Q_{2,0},Q_{2,1},...,Q_{2,n-1}\right\}^T \quad (19)$$

The DPM used for comparison was developed using ANSYS Fluent. This ensures the validity of the comparisons and the verification of HM-AN of LPM.

3. THEORETICAL ANALYSIS

3.1 LAPACE TRANSFORM

The Laplace transform is a powerful integral transform widely used in various fields, notably in automatic industrial control theory. It facilitates the derivation of a transfer function from a given equation, mapping the relationship between input and output. In this paper, we applied Laplace transforms to three distinct models, highlighting subtle differences in the transfer functions of each (see Table 1). These differences are further illustrated through numerical simulations presented in the subsequent section.

From Eq. (12), (13), and (14), the input-output fluid temperature, denoted as *Wη(s)*, is derived using the Laplace transform as follows:

$$W_\eta(s)=\frac{\frac{\alpha_d T_m e^{-\alpha_d}}{1-e^{-\alpha_d}}s+1}{\tau_0 T_m s^2+\left(\tau_0+\frac{\alpha_d T_m}{1-e^{-\alpha_d}}\right)s+1} \quad (20)$$

The input-output heat transfer function *Wq (s)* is

$$W_q(s)=\frac{1}{\tau_0 T_m s^2+\left(\tau_0+\frac{\alpha_d T_m}{1-e^{-\alpha_d}}\right)s+1} \quad (21)$$

The input-output fluid velocity function *Wd (s)* is

$$W_d(s)=\frac{\frac{(1-n)\alpha_d T_m e^{-\alpha_d}}{(1-e^{-\alpha_d})^2}s+1}{\tau_0 T_m s^2+\left(\tau_0+\frac{\alpha_d T_m}{1-e^{-\alpha_d}}\right)s+1} \quad (22)$$

The transfer functions characterizing the relationships between input-output fluid temperature, heat transfer, and fluid velocity within the DPM are presented in the following forms:

`

$$\overline{W}_{\eta}(s)=\exp\left(-\tau_0 s-\frac{\alpha_d T_m s}{1+T_m s}\right) \quad (23)$$

$$\overline{W}_{q}(s)=\frac{1-\overline{W}_{\eta}}{\tau_0 T_m s^2+(\tau_0+\alpha_d T_m)s} \quad (24)$$

$$\overline{W}_{d}(s)=-\frac{(1+(1-n)T_m s)(1-\overline{W}_{\eta})}{\tau_0 T_m s^2+(\tau_0+\alpha_d T_m)s} \quad (25)$$

For the LPM, the transfer functions for input-output fluid temperature, heat transfer, and fluid velocity are given as follows:

$$\hat{W}_{\eta}(s)=\frac{T_m s+1}{\tau_0 T_m s^2+(T_m+\tau_0+\alpha_d T_m)s+1} \quad (26)$$

$$\hat{W}_{q}(s)=\frac{1}{\tau_0 T_m s^2+(T_m+\tau_0+\alpha_d T_m)s+1} \quad (27)$$

$$\hat{W}_{\eta}(s)=\frac{(1-n)T_m s+1}{\tau_0 T_m s^2+(T_m+\tau_0+\alpha_d T_m)s+1} \quad (28)$$

3.2 THEORETICAL ERROR ANALYSIS

In the realm of thermal engineering theory, the method of time domain analysis is employed to compare and scrutinize the dynamic characteristics of systems. By conducting a Taylor expansion of the transfer function around the point $s\to 0$ or $s\to\infty$ and leveraging the initial/final value theorem of Laplace transform, we find that the results align across the three models.

The Taylor expansion for formulas (26) to (28) at $s=0$ is performed. Upon disregarding higher-order terms, the simplified expansions of the input-output temperature transfer functions for the three models are derived as follows:

$$\overline{W}_{\eta}(s)=1-(\tau_0+\alpha_d T_m)s+\frac{(\tau_0+\alpha_d T_m)^2+2\alpha_d T_m{}^2}{2!}s^2+O(s^2) \quad (29)$$

$$W_{\eta}(s)=1-(\tau_0+\alpha_d T_m)s+\frac{(\tau_0+\alpha_d T_m)^2+2\alpha_d T_m{}^2+\tau_0-\alpha_d{}^2 T_m{}^2}{2!}s^2+O(s^2) \quad (30)$$

$$\hat{W}_{\eta}(s)=1-(\tau_0+\alpha_d T_m)s+\frac{(\tau_0+\alpha_d T_m)^2+2\alpha_d T_m{}^2+(\tau_0+\alpha_d T_m)^2}{2!}s^2+O(s^2) \quad (31)$$

The transfer functions for input-output heat across the three models are detailed below, providing insights into the heat dynamics within each system.

$$\overline{W}_{q}(s)=1-(\frac{\tau_0+\alpha_d T_m}{2}+T_m)s+O(s) \quad (32)$$

$$W_{q}(s)=1-(\tau_0+\frac{\alpha_d T_m}{1-e^{-\alpha_d}})s+O(s)\approx 1-(\frac{\tau_0+\alpha_d T_m}{2}+T_m+\frac{\tau_0-\alpha_d T_m}{2})s+O(s) \quad (33)$$

$$\hat{W}_{q}(s)=1-(\tau_0+\alpha_d T_m+T_m)s+O(s)=1-(\frac{\tau_0+\alpha_d T_m}{2}+T_m+\frac{\tau_0+\alpha_d T_m}{2})s+O(s) \quad (34)$$

`

Similarly, the transfer functions for input-output fluid velocity for the three models are presented, highlighting the variations in fluid dynamics.

$$\overline{W}_d(s) = -1 + (\frac{\tau_0 + \alpha_d T_m}{2} + nT_m)s + O(s) \quad (35)$$

$$\begin{aligned} W_d(s) &= -1 + \left(-\frac{(1-n)\alpha_d{}^2 T_m e^{-\alpha_d}}{(1-e^{-\alpha_d})^2} + \tau_0 + \frac{\alpha_d T_m}{1-e^{-\alpha_d}} \right) s + O(s) \\ &\approx -1 + \left(\frac{\tau_0 + \alpha_d T_m}{2} + nT_m + \frac{\tau_0 - (2n-1)\alpha_d T_m}{2} \right) s + O(s) \end{aligned} \quad (36)$$

$$\hat{W}_d(s) = -1 + (\frac{\tau_0 + \alpha_d T_m}{2} + nT_m + \frac{-\tau_0 + \alpha_d T_m}{2})s + O(s) \quad (37)$$

Subsequently, the transfer functions from the HM-AN, LPM, and DPM are compared. The results for the input-output temperature transfer function are as follows:

$$\left| W_\eta(s) - \overline{W}_\eta(s) \right| = \left| \frac{\tau_0 - \alpha_d{}^2 T_m{}^2}{2!} \right| < \left| \frac{(\tau_0 + \alpha_d T_m)^2}{2!} \right| = \left| \hat{W}_\eta(s) - \overline{W}_\eta(s) \right| \quad (38)$$

For the transfer function of input-output heat, the comparative results across the models are presented:

$$\left| W_q(s) - \overline{W}_q(s) \right| = \left| \frac{\alpha_d T_m - \tau_0}{2} \right| < \left| \frac{\alpha_d T_m + \tau_0}{2} \right| = \left| \hat{W}_q(s) - \overline{W}_q(s) \right| \quad (39)$$

For the transfer function of input-output fluid velocity, assuming a fluid velocity factor of n=0.8, the comparative results are as follows:

$$\left| W_d(s) - \overline{W}_d(s) \right| = \left| \frac{0.6\alpha_d T_m - \tau_0}{2} \right| < \left| \frac{\alpha_d T_m - \tau_0}{2} \right| = \left| \hat{W}_d(s) - \overline{W}_d(s) \right| \quad (40)$$

The analysis underscores that the HM-AN aligns more closely with the DPM than with the LPM, indicating its enhanced capability in capturing the dynamics of the system.

4. RESULTS

4.1 SIMULATION CONDITIONS

In current simulation studies, LPM is considered a viable method, and the differential equations are typically solved using the Runge-Kutta method [34]. In LPM, physical parameters such as the temperatures inside and outside the tube are represented by a single typical point. The working fluid's inlet and outlet parameters are represented by the arithmetic mean values at these typical points. The former is chosen for ease of calculating heat transfer to the working fluid within the heated tubes, while the latter is selected to describe variations in fluid parameters, such as mass flow. However, it is important to note that LPM inherently lacks the ability to display parameter variations along the tubes, a capability that DPM possesses. Despite this limitation, LPM provides sufficiently accurate results, especially in steady-state studies.

`

The boundary conditions play a critical role in solving the governing equations and ensuring accurate simulation results. For the Fluent model (see Fig. 3), the inlet boundary condition is defined as a mass-flow-inlet, the outlet boundary condition is set as a pressure-outlet, and the thermal boundary condition on the outer wall of the heated pipe is specified as a constant heat flux. These conditions allow for the accurate representation of heat transfer and fluid flow dynamics within the pipe. For HM-AN and LPM, implemented independently using C++ programming, the working pressure, inlet mass flow rate, inlet temperature, and heat flux are directly input into the model calculation functions. These boundary conditions are consistent across all models to ensure comparability. The simulation process begins with steady-state calculations to establish baseline conditions, followed by transient simulations where step disturbances in inlet temperature, mass flow rate, and heat flux are applied to evaluate the dynamic response of the system. This detailed treatment of boundary conditions ensures that the models accurately capture the physical behavior of the system under both steady-state and transient conditions.

A theoretically verified approach enables reliable modeling of heated pipe systems and simulating transient responses before actual operation [16]. Advances in LPM now allow dynamic calculation of key parameters for supercritical fluids in boiler-turbine systems [18], while DPM has been developed for subcritical coal-fired boilers [35]. Further mathematical studies cover thermal hydraulics in ultra-supercritical boilers [36-37] and advanced simulating techniques using AI and fuzzy-neural networks [38-391]. Although mathematical modeling is crucial for power plant simulating, the dynamic response to disturbances is nonlinear, leading to uncertainties and calculation errors due to un-modeled dynamics [40]. Traditional modeling involves dynamic simulations based on fundamental physical and semi-empirical laws, balancing calculation speed and accuracy. This requires validation for both transient and steady-state reliability, along with the need for rapid, economical performance in the optimal simulation system [40-42].

Current studies on fluid and heat dynamic simulating primarily focus on establishing mathematical models based on lumped and distributed parameters. Lumped parameter modeling facilitates simulation due to its fast computation speeds and accelerated convergence [43], though its equation fitting properties are limited in scope, making it challenging to capture detailed information about local features during transient processes. Distributed parameter modeling, on the other hand, relies on establishing 2-D or 3-D models that require extensive numerical calculations to achieve computational accuracy [44-45]. Numerous commercial, in-house, and freeware CFD codes have been developed, with ANSYS Fluent frequently used as a reliable tool for design and optimization in both scientific studies and technological applications [46].

In traditional practice, simulation platforms aim to integrate all reliable sub-models of the working fluid in discretized component parts, enabling dynamic simulation of the entire boiler. Typically, LPM, rather than DPM, proposes a 1-dimensional discretized simplified model for dynamic process simulation, where all equations of mass, momentum, and energy are numerically solved in each discrete unit. As a crucial aspect of modeling boiler systems, SFHPs play a significant role in the heated surfaces of power plant boilers, and mathematical modeling of SFHPs remains a pivotal research topic in the simulation field of power plants. Over the past decades, numerous models of SFHPs have been established [47-49], exploring optimal solutions between accuracy and convergence rate.

`

The single-phase heated pipe in this validation case has a length of 27,610 mm, an outer diameter of 38 mm, and a wall thickness of 5.5 mm. In the Fluent simulation, the pipe was divided into two regions: the pipe wall (metal) and the working fluid (internal flow). A fully coupled mesh was used at the interface to compute heat transfer between the two regions. The pipe wall was divided into three radial layers to account for the temperature gradient, while the fluid region included a five-layer boundary layer near the wall to capture velocity gradients, with thicknesses increasing radially by a factor of 1.2 up to 2 mm. The remaining fluid region was meshed with tetrahedral elements, and both regions were divided into 5,000 axial segments to align the mesh nodes at the interface. The computational mesh consisted of 480,000 control volumes and 640,128 nodes for the pipe wall, and 1,250,000 control volumes and 1,335,267 nodes for the fluid region.The specific boundary parameters for the validation case included a pressure of 26.7 *MPa*, a mass flow rate of 0.3739 *kg/s*, inlet temperatures of 553.15 *K* for water and 743.15 *K* for steam, and heat fluxes of 30,185.75 W/m^2 for water and 35,760.14 W/m^2 for steam. Additionally, transient simulations were performed by introducing step changes of +10% in the inlet mass flow rate, +10 *K* in the inlet temperature, and +10% in the heat flux.

4.2 SIMULATION RESULTS

After confirming the consistency of steady-state values with three theoretical models, we simulated the dynamic behavior of a heated tube subjected to disturbances such as changes in mass flow rate, inlet fluid temperature, and external heat duty from fuel gas. In simulating systems, regulating operational conditions in response to load variations is crucial. In this study, disturbances were represented by variations in mass flow rate, inlet fluid temperature, and heat duty, which correspond to changes in feed water conditions and fuel supply rates, respectively.

For a detailed analysis of how the three models perform under variable working conditions, we selected the super-heater of an ultra-supercritical boiler as the simulation subject. The models were set with a pressure of 26.7 *MPa*, a mass flow of 0.3739 *kg/s*, an inlet water temperature of 553.15 *K*, and a heat flow of 30185.75 W/m^2. The characteristic parameters were τ_0 = 4.0 s and T_m = 21.8 s. The dynamic simulation results of the three models are compared in Fig. 4.

Fig. 4(a) illustrates the dynamic process of outlet water temperature when the inlet water temperature was disturbed by a 10K increase. After 140 seconds, the three models approached a steady state, showing consistent results for outlet water temperature. Despite the increase in inlet water temperature, the outlet water temperature initially remained nearly constant, a delay consistent with the actual operation due to the tube-wall's length from inlet to outlet. Among the three models, the hybrid model consistently produced results between those of the LPM and the DPM, indicating that it aligns closely with the ANSYS Fluent results.

Fig. 4(b) displays the dynamics when the inlet water flow mass was increased by 10%. The outlet water temperature is observed to decrease over time, eventually stabilizing. The hybrid model's simulation results again closely matched those of the DPM calculated by ANSYS Fluent, more so than the LPM.

Fig. 4(c) shows the response to a 10% increase in external heat duty. Initially, the hybrid model's curve resembled that of the LPM but aligned more closely with the DPM as it approached steady state. Overall, the steady-state results of the LPM and hybrid model were consistent with the DPM, but the dynamic behavior of the hybrid model was intermediary between the LPM and DPM. This suggests

`

that, with the same number of tube units (N=5), the hybrid model's calculations more closely resemble those of the DPM.

To further validate the hybrid model's rationality, this paper compares dynamic curves from the three models by dividing the tube into three units, using steam as the working medium. The thermo-physical properties of steam, which vary with temperature, were set differently in each unit. Given that ANSYS Fluent simulations are generally considered highly accurate—despite longer computation times—it was used as the benchmark DPM. The super-heater of an ultra-supercritical boiler was again the simulation subject, with a time step of 0.1s. The conditions were set to a pressure of 26.7MPa, a mass flow of 0.3739kg/s, an inlet steam temperature of 743.13K, and a heat flow of 35760.14W/m^2.

From Fig. 5(a), there is a noticeable temperature rise with a time delay when the inlet steam temperature was disturbed by a 10K increase, observable in both the distributed parameter and hybrid models, but not in the lumped parameter model with N=3.

Fig. 5(b) and 5(c) show the dynamic processes of outlet steam temperature when the inlet steam flow mass and external heat duty were increased by 10%, respectively. Although differences exist among the dynamic curves of the three models, the hybrid model's results were superior to those of the LPM and more closely resembled the ANSYS Fluent simulation results.

The real-time simulation results of the proposed HM-AN provide significant physical insights into the heat transfer and fluid flow dynamics within single-phase heated pipes. Unlike traditional LPM, the HM-AN model dynamically couples the heat transfer rates with the fluid and wall temperatures, capturing transient phenomena such as transport delays and thermal inertia. This coupling ensures that the model reflects the physical reality of heat transfer processes more accurately, particularly under transient conditions, such as step changes in inlet temperature, flow rate, or external heat flux.

The comparison with ANSYS Fluent results highlights the differences in focus between the two approaches. ANSYS Fluent, as a high-fidelity DPM, provides detailed spatial distributions of temperature, velocity, and turbulence parameters across the computational domain. This level of detail is essential for understanding localized phenomena, such as boundary layer development and turbulence effects. However, the computational intensity of Fluent makes it unsuitable for real-time applications.

In contrast, the HM-AN model simplifies the spatial resolution by dividing the pipe into finite segments with uniform or linearly varying physical properties. This approach sacrifices some spatial detail but achieves rapid convergence and computational efficiency, making it ideal for real-time simulation. Despite these differences in focus, the results of the HM-AN model align closely with those of Fluent in terms of key outputs, such as outlet temperature and dynamic responses to step changes. This agreement demonstrates the ability of the HM-AN model to capture the essential physics of the system while maintaining computational efficiency.

For example, the improved response of the HM-AN model to step changes in inlet temperature can be attributed to its ability to account for transport delay, which depends on pipe length and fluid velocity. This phenomenon is often overlooked in traditional LPMs but is accurately captured by the proposed model. Similarly, the dynamic coupling of heat transfer with fluid and wall temperatures enhances the accuracy of the model's response to variations in inlet flow rate and external heat flux.

`

These results are consistent with ANSYS Fluent simulations, confirming the validity of the proposed model while emphasizing its suitability for real-time industrial applications.

5. CONCLUSIONS

This paper introduces a novel method for modeling the dynamics simulation in convective heated surfaces of SFHPs. The proposed method involves solving the mass, energy, and continuity equations within a one-dimensional framework, utilizing an explicit acceleration solution. In this HM-AN approach, boundary conditions are adjustable, accounting for external heat duty and a time-dependent internal heat release, rather than the traditional constant value. Computations are executed along the flow path of the heated medium, either in a single or in consecutive tube units.

Initial and steady-state values of lumped parameters, distributed parameters, and hybrid models align in the dynamic process following a disturbance. Thus, it is essential to compare the errors in the dynamic process between the hybrid model and the LPM theoretically. The introduction of Laplace transforms in the three models highlights subtle differences in their transfer functions. Through Taylor expansion and the omission of higher-order terms, analysis indicates that the hybrid model aligns more closely with the DPM than with the LPM.

Given the need for SFHPs to adapt to varying thermal load conditions, operational simulations of the three models were conducted under specific disturbances in input temperature, flow mass, and heat duty. Utilizing the highly reliable CFD simulation of ANSYS Fluent software as a reference for DPM, we compared the dynamic response curves of the hybrid model with those of the LPM. The super-heater of an ultra-supercritical boiler was selected as the simulation object for the SFHP, with water as the working medium in a system divided into five tube units. Results showed that the hybrid model's calculations more closely resembled those of the DPM, displaying characteristic time-delay responses at the onset of disturbances. Furthermore, during the dynamic process, the curve approximation of the hybrid model was nearly consistent with the ANSYS Fluent results.

Additionally, the results demonstrated that the accuracy of the hybrid model surpassed that of the LPM, also reflecting the systemic characteristics of a time-delay in response to disturbances. This hybrid model could be effectively applied in the design of real-time simulating systems.

FUNDING

The presented study is performed by National Nature Science Foundation of China (No. 51875100).

CONFLICT OF INTEREST

The authors declare that they have no conflicts of interest.

`

REFERENCES

1. Wehbia, Z., Taherb, R., Faraja, J., et al. “Waste water heat recovery systems types and applications: Comprehensive review, critical analysis, and potential recommendations”, *Energy Rep.* **9**, pp. 16–33 (2023). https://doi.org/10.1016/j.egyr.2023.05.243
2. Inayat, A. “Current progress of process integration for waste heat recovery in steel and iron industries”, *Fuel* **338**, 127237 (2023). https://doi.org/10.1016/j.fuel.2022.127237
3. Xu, Z., Gao, J., Mao, H., et al., “Double-section absorption heat pump for the deep recovery of low-grade waste heat”, *Energy Convers. Manag.* **220**, 113072 (2020). https://doi.org/10.1016/j.enconman.2020.113072
4. Jiang, L., Li, Y., Yao, Y. et al. “Heat transfer and protection of high-temperature reheater of a 660 MW circulating fluidized bed boiler after black out”, *Appl. Therm. Eng.* **213**, 118654 (2022). https://doi.org/10.1016/j.applthermaleng.2022.118654
5. Xu, H., Deng, B., Jiang, D., et al. “The finite volume method for evaluating the wall temperature profiles of the superheater and reheater tubes in power plant”, *Appl. Therm. Eng.* **112**, pp. 362-370 (2017). http://dx.doi.org/10.1016/j.applthermaleng.2016.10.091
6. Modlinski, N. and Janda, T. “Mathematical procedure for predicting tube metal temperature in the radiant superheaters of a tangentially and front fired utility boilers”, *Therm. Sci. Eng. Prog.* **40,** 101763 (2023). https://doi.org/10.1016/j.tsep.2023.101763
7. Abdelsalam, E., Abu El-Rub, Z., Alkasrawi, M., et al., “A novel design of a twin-chimney solar power plant for power and distilled water production”, *Therm. Sci. Eng. Prog.* **46**, 102231 (2023). https://doi.org/10.1016/j.tsep.2023.102231
8. Sadeghzadeh, M., Ghorbani, B., Ahmadi, M. H., et al., “Process diagram of the proposed plant to supply power, cooling, freshwater, and hot water for an industrial complex”, *Energy Rep.* **7**, pp. 5344-5358 (2021). https://doi.org/10.1016/j.egyr.2021.08.168
9. Abdel-Dayem, A. M., and Hawsawi, Y. M. “Feasibility study using TRANSYS modelling of integrating solar heated feed water to a cogeneration steam power plant”, *Case Stud. Therm. Eng.* **39**, 102396 (2022). https://doi.org/10.1016/j.csite.2022.102396
10. Adhikari, N., Bhandari, R., and Joshi, P. “Thermal analysis of lithium-ion battery of electric vehicle using different cooling medium”, *Appl. Energy* **360**, 122781 (2024). https://doi.org/10.1016/j.apenergy.2024.122781
11. Hwang, F. S., Confrey, T., Reidy, C., et al. “Review of battery thermal management systems in electric vehicles”, *Renew. Sustain. Energy Rev.* **192**, 114171 (2024). https://doi.org/10.1016/j.rser.2023.114171
12. Lei, S., Xin, S., and Liu, S. “Separate and integrated thermal management solutions for electric vehicles: A review”, J. Power Sources **550**, 232133 (2022). https://doi.org/10.1016/j.jpowsour.2022.232133
13. Song, P., An, Z., Wei, M., Sun, et al. “Cooling performance and optimization of a thermal management system based on CO_2 heat pump for electric vehicles”, *Energy Convers. Manag.* **306**, 118299 (2024). https://doi.org/10.1016/j.enconman.2024.118299

`

14. Yerasimou,Y., Werner, T.C., and Pickert, V. “On the application of liquid metal cooling for electronic switching devices”, *Therm. Sci. Eng. Pro.* **42**, 101875 (2023). https://doi.org/10.1016/j.tsep.2023.101875
15. Chu, Y.M., Farooq, U., Mishra, N. K. et al. “CFD analysis of hybrid nanofluid-based microchannel heat sink for electronic chips cooling: Applications in nano-energy thermal devices”, *Case Stud. Therm. Eng.* **44**, 102818 (2023). https://doi.org/10.1016/j.csite.2023.102818
16. Di Capua, M.H., and Jahn, W. “Performance assessment of thermoelectric self-cooling systems for electronic devices”, *Appl. Therm. Eng.* **193**, 117020 (2021). https://doi.org/10.1016/j.applthermaleng.2021.117020
17. Muneeshwaran, M., Lin, Y.-C., and Wang, C.-C. “Performance analysis of single-phase immersion cooling system of data center using FC-40 dielectric fluid”, *Int. Commun. Heat Mass Transf.* **145**, 106843 (2023). https://doi.org/10.1016/j.icheatmasstransfer.2023.106843
18. Awais, M., Ullah, N., Ahmad, J., et al. “Heat transfer and pressure drop performance of Nanofluid: A state-of-the-art review”, *Int. J. Thermofluids* **9**, 100065 (2021).https://doi.org/10.1016/j.ijft.2021.100065
19. Awais, M., Bhuiyan, A.A., Salehin, S., et al. “Synthesis, heat transport mechanisms and thermophysical properties of nanofluids: A critical overview”, *Int. J. Thermofluids* **10**, 100086 (2021). https://doi.org/10.1016/j.ijft.2021.100086
20. Ahmad, F., Mahmud, S., Ehsan, M.M., et al. “Thermo-hydrodynamic performance evaluation of double-dimpled corrugated tube using single and hybrid nanofluids”, *Int. J. Thermofluids* **17**, 100283 (2023). https://doi.org/10.1016/j.ijft.2023.100283
21. Ahamed, R., Salehin, M., and Ehsan, M.M. “Thermal-hydraulic performance and flow phenomenon evaluation of a curved trapezoidal corrugated channel with E-shaped baffles implementing hybrid nanofluid”, *Heliyon* **10** (7), e28698 (2024). https://doi.org/10.1016/j.heliyon.2024.e28698
22. Ahmad, F., Mahmud, S., Ehsan, M.M., et al. “Numerical Assessment of Nanofluids in Corrugated Minichannels: Flow Phenomenon and Advanced Thermo-hydrodynamic Analysis”, *Int. J. Thermofluids* **20** (2023). https://doi.org/10.1016/j.ijft.2023.100449
23. Mustakim, A., Islam, S.M.N.U., Ahamed, R., et al. “Numerical Assessment of Advanced Thermo-Hydrodynamic Characteristics of Nanofluid Inside a Helically Featured Straight Pipe”, *Int. J. Thermofluids* **21**, 100591 (2024). https://doi.org/10.1016/j.ijft.2024.100591
24. Islam, S.M.N.U., Mustakim, A., Ahamed, R., et al. “Advanced Thermo-Hydraulic Assessment of Helical Pipes with Different Shapes of Jackets Using Single-Phase and Hybrid Nanofluids”, *Int. J. Thermofluids* **22**, 100628 (2024). https://doi.org/10.1016/j.ijft.2024.100628
25. Awais, M., Saad, M., Ayaz, H., et al. “Computational assessment of Nano-particulate (Al_2O_3/Water) utilization for enhancement of heat transfer with varying straight section lengths in a serpentine tube heat exchanger”, *Therm. Sci. Eng. Prog.* **20**, 100521 (2020). https://doi.org/10.1016/j.tsep.2020.100521
26. Porgar, S., Huminic, G., Huminic, A., et al. “Application of nanofluids in heat exchangers - A state-of-the-art review”, *Int. J. Thermofluids* **24**, 100945 (2024). https://doi.org/10.1016/j.ijft.2024.100945

`

27. Alhulaifi, A.S. “Numerical characterization of the performance of counter-flow double-pipe heat exchanger using nanofluids for laminar flow regime”, *Results Eng.* **25**, 104061 (2025). https://doi.org/10.1016/j.rineng.2025.104061
28. Kadhim, S.A., Hammoodi, K.A., Askar, A.H., et al. “Feasibility review of using copper oxide nanofluid to improve heat transfer in the double-tube heat exchanger”, *Results Eng.* **24**, 103227 (2024). https://doi.org/10.1016/j.rineng.2024.103227
29. Zima, W. “Simulation of rapid increase in the steam mass flow rate at a supercritical power boiler outlet”, *Energy* **173**, 995-1005 (2019). https://doi.org/10.1016/j.energy.2019.02.127
30. Adams, J., Clark, D. R., Louis, J. R. et al., “Mathematical modeling of once-through boiler dynamics”, *IEEE Trans. Power App. Syst.* **84**(2), 146-156 (1965). https://doi.org/10.1109/TPAS.1965.4766165
31. Kicsiny, R. “New delay differential equation models for heating systems with pipes”, *Int. J. Heat Mass Transf.* **79**, 807-815 (2014). http://dx.doi.org/10.1016/j.ijheatmasstransfer.2014.08.058
32. Wurm, J., Bachler, S., Woittennek, F., et al. “On delay partial differential and delay differential thermal models for variable pipe flow”, *Int. J. Heat Mass Transf.* **152**, 119403 (2020). https://doi.org/10.1016/j.ijheatmasstransfer.2020.119403
33. Pekař, L., Matušů, R., Dostálek, P., et al. “Further experimental results on modelling and algebraic control of a delayed looped heating-cooling process under uncertainties”, *Heliyon* **9**(8), e18445 (2023). https://doi.org/10.1016/j.heliyon.2023.e18445
34. Pan, J., Yang, D., Chen, G., et al. “Thermal-hydraulic analysis of a 600 MW supercritical CFB boiler with low mass flux”, *Appl. Therm. Eng.* **32**, 41-48 (2012). https://doi.org/10.1016/j.applthermaleng.2011.08.009
35. Zheng, S., Luo, Z., Zhang, X., et al. “Distributed parameters modeling for evaporation system in a once-through coal-fired twin-furnace boiler”, *Int. J. Therm. Sci.* **50**(12), 2496-2505 (2011). https://doi.org/10.1016/j.ijthermalsci.2011.07.010
36. Pan, J., Wu, G., Yang, D., et al. “Thermal-hydraulic calculation and analysis on water wall system of 600 MW supercritical CFB boiler”, *Appl. Therm. Eng.* **82**, 225-236 (2015). https://doi.org/10.1016/j.applthermaleng.2015.03.004
37. Zhu, X., Wang, W., Xu, W., et al. “A study of the hydrodynamic characteristics of a vertical water wall in a 2953t/h ultra-supercritical pressure boiler”, *Int. J. Heat Mass Transf.* **86**, 404-414 (2015). https://doi.org/10.1016/j.ijheatmasstransfer.2015.03.010
38. Chaibakhsh, A., Ghaffari, A., Moosavian, S.A.A., et al. “A simulated model for a once-through boiler by parameter adjustment based on genetic algorithms”, *Simul. Model. Pract. Theory* **15**(9), 1029-1051 (2007). https://doi.org/10.1016/j.simpat.2007.06.004
39. Liu, X.J., Kong, X.B., Hou, G.L., et al. “Modeling of a 1000 MW power plant ultra super-critical boiler system using fuzzy-neural network methods”, *Energy Convers. Manage.* **65**, 518-527 (2013). https://doi.org/10.1016/j.enconman.2012.07.028
40. Weng, C.K., Ray, A., Xiaowen, D., et al. “Modelling of power plant dynamics and uncertainties for robust control synthesis”, *Appl. Math. Model.* **20**(7), 501-512 (1996). https://doi.org/10.1016/0307-904x(95)00169-k
41. Demello, F. P. “Boiler models for system dynamic performance studies”, *IEEE Power Eng. Rev.* **11**, 47 (1991). https://doi.org/10.1109/MPER.1991.88720

`

42. Zhang, H., Gao, M., Yu, H., et al. “A dynamic nonlinear model used for controller design of a 600 MW supercritical circulating fluidized bed boiler-turbine unit”, *Appl. Therm. Eng.* **212**, 118547 (2022). https://doi.org/10.1016/j.applthermaleng.2022.118547
43. Taler, J., Zima, W., Ocłoń, P., et al. “Mathematical model of a supercritical power boiler for simulating rapid changes in boiler thermal loading”, *Energy* **175**, 580-592 (2019). https://doi.org/10.1016/j.energy.2019.03.085
44. Wang, Y., Cao, L., Li, X., et al. “A novel thermodynamic method and insight of heat transfer characteristics on economizer for supercritical thermal power plant”, *Energy* **191**, 116573 (2020). https://doi.org/10.1016/j.energy.2019.116573
45. Modliński, N., Szczepanek, K., Nabagło, D., et al. “Mathematical procedure for predicting tube metal temperature in the second stage reheater of the operating flexibly steam boiler”, *Appl. Therm. Eng.* **146**, 854-865 (2019). https://doi.org/10.1016/j.applthermaleng.2018.10.063
46. Adamczyk, W. P. “Application of the numerical techniques for modelling fluidization process within industrial scale boilers”, *Arch. Comput. Methods Eng.* **24**(4), 669-702 (2017). https://doi.org/10.1007/s11831-016-9186-z
47. Enns, M. “Comparison of dynamic models of a superheater”, *J. Heat Trans-T ASME* **84**, 375-382 (1962). https://doi.org/10.1115/1.3684401
48. Wang, H., and Che, D. “Positive flow response characteristic in vertical tube furnace of supercritical once-through boiler”, *J. Therm. Sci. Eng. Appl.* **6**(3), 031102-031114 (2014). https://doi.org/10.1115/1.4025945
49. Zhang, Q., Wang, Z., Du, X., et al. “Dynamic simulation of steam generation system in solar tower power plant”, *Renew. Energy* **135**, 866-876 (2019). https://doi.org/10.1016/j.renene.2018.12.064

`

Nomenclature

A_2	Internal surface area of tube (m^2)
c_j	Wall specific heat ($kJ / kg\ K$)
c_p	Specific heat of fluid ($kJ / kg\ K$)
c_{p0}	Specific heat of fluid at steady state ($kJ / kg\ K$)
d_2	Internal diameter of tube (m)
D	Mass flow (kg / s)
D_0	Mass flow at steady state (kg / s)
D_{in}	Input fluid mass flow (kg / s)
F	Area of cross-section (m^2)
h	Enthalpy of fluid (kJ / kg)
L	Length of tube (m)
m_j	Wall mass per unit length (kg / m)
M_j	Wall mass (kg)
N	Numbers of control body
p	Pressure of fluid (MPa)
p_d	Pressure losss per unit length (MPa / m)
q_1	External heat flow per unit length (kW / m)
Q_1	External heat flow (kW)
Q_{10}	External heat flow at steady state (kW)
q_2	Internal heat flow per unit length (kW / m)
Q_2	Internal heat flow (kW)
Q_{20}	Internal heat flow at steady state (kW)
T	Fluid temperature (K)
T_{in}	Inlet temperature of fluid (K)
T_{in0}	Inlet temperature of fluid at steady state (K)
T_j	Wall temperature (K)
T_{j0}	Wall temperature at steady state (K)
T_m	Heat storage time constant of metal tube-wall (s)
T_{out}	Outlet temperature of fluid (K)
T_{out0}	Outlet temperature of fluid at steady state (K)
U_2	Inner circumference of tube (m)
z	Axial unit length (m)

Greek Symbols

ρ	Density of fluid (kg / m^3)
ω	Velocity of flow (m / s)
ω_0	Velocity of flow at steady state (m / s)
α_2	Heat transfer coefficient of the inner wall to fluid (kW / m^2K)
α_{20}	Heat transfer coefficient of the inner wall to fluid at steady state (kW / m^2K)
τ	Time (s)
τ_0	Flow time (s)

Subscript

i	Index of control body
p	Constant pressure
T	Constant temperature

Dimensionless parameter

K_2	Ratio of heat transfer coefficient to nth power of mass flow
n	nth power of mass flow
α_d	Dynamic parameter

`

Table 1 Transfer Function Sheet

Parameter	Formula
Heat release coefficient in tube in steady state	$\alpha_{20} \approx K_2 D_0^n$
Heat storage time constant of metal tube-wall	$T_m = \frac{m_j c_j}{\alpha_{20} U_2} = \frac{M_j c_j}{\alpha_{20} A_2}$
Dynamic parameter	$a_d = \frac{\alpha_{20} A_2}{D_0 c_p}$
Flow time	$\tau_0 = \frac{L}{\omega_0}$

`

FIGURE CAPTIONS

Fig. 1. The schematic diagram of working principle of a SFHP.

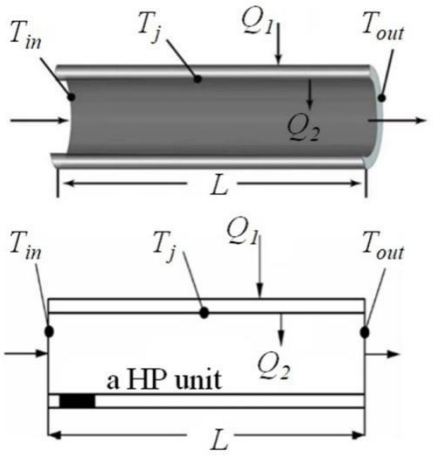

Fig. 2. The schematic diagram of working principle of one segment of SFHP unit, considering physical property change.

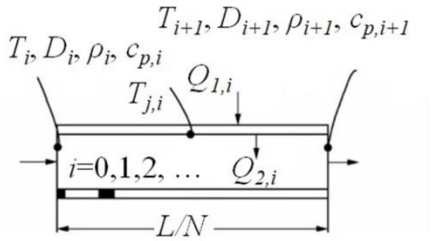

Fig. 3. The geometry modeling of a SFHP in DPM. The algorithm of ANSYS Fluent is SIMPLE (Semi-Implicit Method for Pressure-Linked Equations). Unlike LPM, DPM not only deals with the working fluid and the innner wall in details, but also takes into account thickness of the wall and its heat transfer.

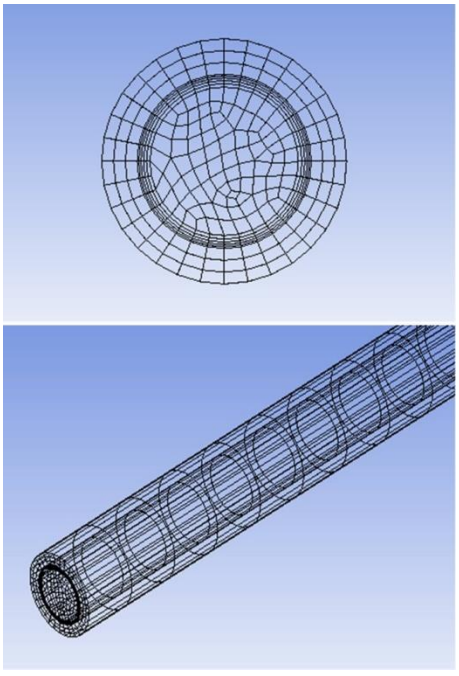

`

Fig. 4. Dynamic curves of output water (as liquid) temperature change by the step disturbance of input parameters. (a) The dynamic curve of output water temperature when the input temperature rise is 10K. (b) The dynamic curve of output water temperature with 10% step increase of input flow mass. (c) The dynamic curve of output water temperature with step of 10% increase of outside heat-duty. Of the three figures, DPM and HM-AN (a) shows the delay characteristics of the system. The curves showed the accuracy of HM-AN is superior to LPM.

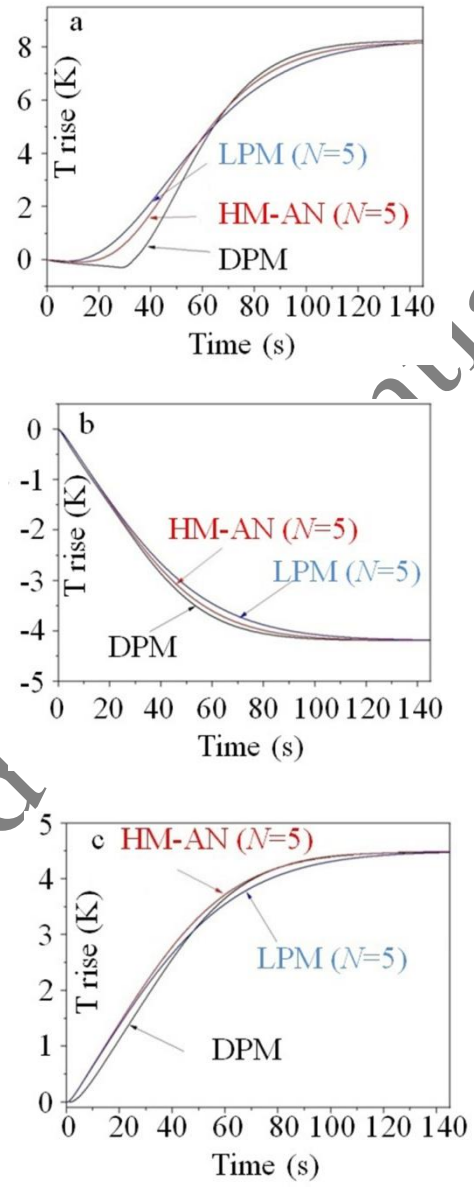

`

Fig. 5. Dynamic curves of output steam (as gas) temperature change of input parameters by the step disturbance. (a) The dynamic curve of output steam temperature when the input temperature rise is 10K. (b) The dynamic curve of output steam temperature with 10% step increase of input flow mass. (c) The dynamic curve of output steam temperature with step of 10% increase of outside heat duty. Of the three figures, DPM and HM-AN (a) shows the delay characteristics of the system. The accuracy of HM-AN is superior to LPM.

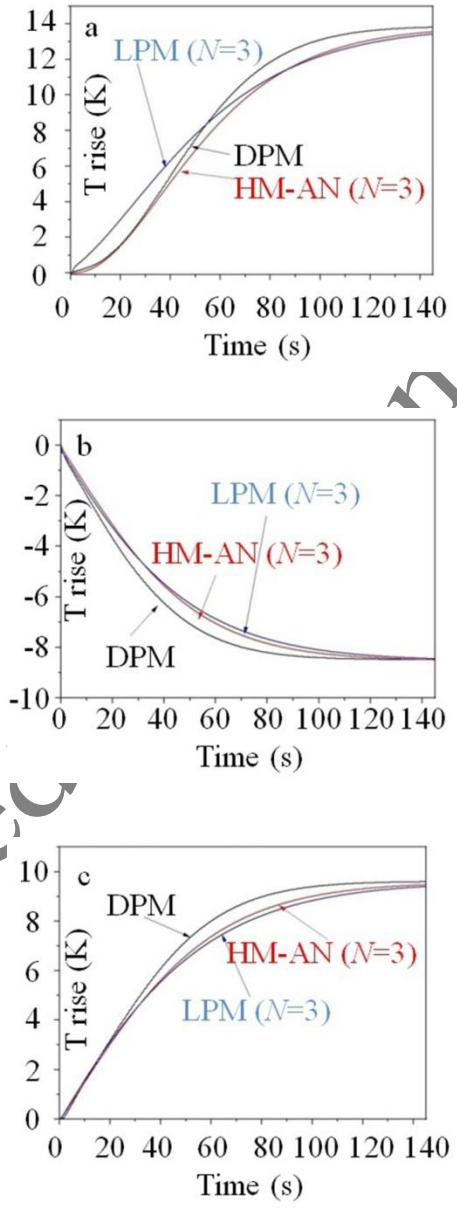

`

Technical Biography

1.

Baoxiang Zhang is a Senior Engineer whose research focuses on energy conservation, emission reduction, and the advancement of smart power plants. He has led and successfully completed several scientific and technological projects, including the development and application of multi-color high colorfastness dope-dyed viscose fiber, intelligent combustion control technology for thermal power pulverized coal boilers, and low-nitrogen combustion technology for medium-temperature circulating fluidized bed boilers.

Author's Address Information
Name: Baoxiang Zhang
Mobile Phone: +86-17731583650
Telephone: +86-03158505291
Email Address: 44151954@qq.com
Postal Address: Tangshan Sanyou Chemical Industries Co., Ltd. Thermal Power Branch, 11 Xingda Road, Nanpu Development Zone, Caofeidian District, Tangshan, Hebei Province, 063020, China

2.

Haifeng Xu is an Engineer specializing in Energy Information Automation at Southeast University, Nanjing, China. He serves as the lead expert in the microgrid and isolated grid application field. He has led and successfully completed several projects, including the Hengyi Brunei Petrochemical large-scale isolated grid project, the Shandong Jingbo Petrochemical short-term isolated grid project, and the Chongqing Huafeng regional power grid project, covering design, consulting, and implementation. He has extensive practical experience in the safe and stable operation of regional and enterprise power grids, frequency regulation and peak shaving of thermal power units, and has achieved outstanding results in the field of microgrid applications.

Author's Address Information
Name: Haifeng Xu
Mobile Phone: +86-13815865169
Telephone: +86- 02568598968
Email Address: xuhf@pkmicrogrid.com
Postal Address: Nanjing Pankong Energy technology Co., Ltd., No. 1266 Qingshuiting East Road, Jiangning District, Nanjing, Jiangsu Province, 211102, China

3.

Hongying Li is a Senior Engineer with extensive experience in the operation and management of power plants. She has led or participated in several scientific and technological projects, including the development and application of low-nitrogen combustion technology for medium-temperature circulating fluidized bed boilers, the research and development of a combined steam and power control system, and the study of intelligent fuel management systems.

`

Author's Address Information
Name: Hongying Li
Mobile Phone: +86-15832599163
Telephone: +86-03158505343
Email Address: 2664554052@qq.com
Postal Address: Tangshan Sanyou Chemical Industries Co., Ltd. Thermal Power Branch, 11 Xingda Road, Nanpu Development Zone, Caofeidian District, Tangshan, Hebei Province, 063020, China

4.

Shuangli Yao is an Engineer specializing in Electrical Engineering and Automation. He has led and successfully completed several scientific and technological projects, including the development and application of low-nitrogen combustion technology for medium-temperature circulating fluidized bed boilers and the development and application of intelligent combustion control technology for thermal power pulverized coal boilers. He has extensive practical experience in ensuring the safety of auxiliary power systems and the long-term operation of boilers in thermal power plants.

Author's Address Information
Name: Shuangli Yao
Mobile Phone: +86-13831550908
Telephone: +86-03158503472
Email Address: 2011338597@qq.com
Postal Address: Tangshan Sanyou Chemical Industries Co., Ltd. Thermal Power Branch, 11 Xingda Road, Nanpu Development Zone, Caofeidian District, Tangshan, Hebei Province, 063020, China

5.

Dr. Xiaohu Xu is a researcher in the School of Energy and Environment at Southeast University, Nanjing, China. He holds a Ph.D. in Power Engineering. His research focuses on performance monitoring of thermal power systems, modeling of carbon emissions and reduction strategies for thermal power units, and the dynamics and simulation of thermal systems. His work spans multiple fields, including coal-fired power, gas-fired power, and nuclear power.

Author's Address Information
Name: Xiaohu Xu
Mobile Phone: +86-13505187691
Telephone: +86-02583792379
Email Address: 101010376@seu.edu.cn
Postal Address: National Engineering Research Center of Power Generation Control and Safety, School of Energy and Environment, No.2 of SEU Road, Jiangning District, Nanjing, Jiangsu Province, 211189, China

`